Raman spectroscopy of substrate-induced compression and substrate doping in thermally cycled graphene

Chun-Chung Chen,[1,*] Wenzhong Bao,[3] Chia-Chi Chang,[2] Zeng Zhao,[3] Chun Ning Lau,[3] and Stephen B. Cronin[1]

[1] *Department of Electrical Engineering, University of Southern California, Los Angeles, California 90089, USA*

[2] *Department of Physics, University of Southern California, Los Angeles, California 90089, USA*

[3] *Department of Physics and Astronomy, University of California, Riverside, Riverside, California 92521, USA*

(Received 27 June 2011; revised manuscript received 16 December 2011; published 20 January 2012)

By thermally cycling single layer graphene in air, we observe irreversible upshifts of the Raman G and $2D$ bands of 24 and 23 cm^{-1}, respectively. These upshifts are attributed to an in-plane compression of the graphene induced by the mismatch of thermal expansion coefficients between the graphene and the underlying Si/SiO_2 substrate, as well as doping effects from the trapped surface charge in the underlying substrate. Since the G and the $2D$ band frequencies have different responses to doping, we can separate the effects of compression and doping associated with thermal cycling. By performing thermal cycling in an argon gas environment and by comparing suspended and on-substrate regions of the graphene, we can separate the effects of gas doping and those of doping from the underlying substrate. Variations in the ratio of the $2D$-to-G band Raman intensities provide an independent measure of the doping in graphene that occurs during thermal cycling. During subsequent thermal cycles, both the G and the $2D$ bands downshift linearly with increasing temperature and then upshift reversibly to their original frequencies after cooling. This indicates that no further compression or doping is induced after the first thermal cycle. The observation of ripple formation in suspended graphene after thermal cycling confirms the induction of in-plane compression. The amplitude and wavelength of these ripples remain unchanged after subsequent thermal cycling, corroborating that no further compression is induced after the first thermal cycle.

DOI: 10.1103/PhysRevB.85.035431 PACS number(s): 65.40.De

I. INTRODUCTION

In the study of graphene, Raman spectroscopy is used widely for identifying the thickness, carrier concentration, temperature, and strain.[1–4] The sensitivity of the Raman G and $2D$ bands to both anharmonic coupling of phonon modes and carbon–carbon length make Raman spectroscopy a useful tool for studying the temperature and strain dependence of graphene.[5–8] Recently, Late *et al.* investigated the Raman spectra of single layer graphene (SLG) on Si/SiO_2 substrates from 77K to 573K and calibrated the temperature coefficient of the G and $2D$ band Raman modes to be $\partial\omega_G/\partial T = -0.016$ cm^{-1}/K and $\partial\omega_{2D}/\partial T = -0.026$ cm^{-1}/K, respectively.[9] Abdula *et al.* also reported temperature coefficients of $\partial\omega_G/\partial T = -0.035$ cm^{-1}/K and $\partial\omega_{2D}/\partial T = -0.07$ cm^{-1}/K for SLG,[10] which are significantly different from those of Late *et al.* Changes in the Raman G and $2D$ bands are also used to estimate the effect of strain in graphene.[11–14] Mohiuddin *et al.* observed strain-induced shifts in the Raman G and $2D$ bands of graphene of $\partial\omega_G/\partial\varepsilon = -58\,cm^{-1}/\%$ and $\partial\omega_{2D}/\partial\varepsilon = -144\,cm^{-1}/\%$, respectively, for graphene under biaxial strain.[15] Ni *et al.* reported $\partial\omega_G/\partial\varepsilon = -14.2\,cm^{-1}/\%$ and $\partial\omega_{2D}/\partial\varepsilon = -27.8\,cm^{-1}/\%$ of Raman G and $2D$ bands, respectively, shift on graphene under uniaxial strain.[6] In addition to temperature and strain, doping causes changes in the Raman spectra.[16] By applying a top gate voltage to SLG, Das *et al.* observed a reduction in the intensity ratio of the $2D$ band to G band. They also observed that the G band frequency upshifts with both n- and p-type doping, whereas the $2D$ band frequency upshifts with p-type doping and downshifts with n-type doping.[17]

While the temperature and strain coefficients of graphene Raman spectra have been reported in many previous works, the effects of strain and doping induced by the underlying substrate are usually not taken into consideration when estimating the Raman temperature coefficient. However, graphene's negative thermal expansion coefficient[18–20] causes a geometric mismatch with most supporting substrates. In addition, graphene is often observed to be doped when the ambient temperature is varied,[21] which implies that the effects of strain and doping cannot be neglected when calibrating the temperature coefficient of the Raman modes of graphene. In this work, we measure the Raman spectra of both suspended and supported graphene before, during, and after thermal cycling from 300 K to 700 K. The Raman G and $2D$ bands are studied systematically. Atomic force microscopy (AFM) is used to determine the suspended graphene profile variation before and after thermal cycling. Thermal cycling in air and Ar gas environments enables us to indentify changes associated with gas doping. In doing so, we are able to separate the effects of doping, compression, and temperature in graphene through the interpretation of the resulting Raman spectra.

II. EXPERIMENTAL METHODS

In this work, graphene flakes are deposited on Si/SiO_2 substrates using mechanical exfoliation.[22,23] The number of graphene layers are identified using Raman spectroscopy by curve fitting the $2D$ band.[24–26] Figure 1(a) and (b) shows an optical microscope image and the Raman spectrum of a single layer graphene flake sample (SLG1) deposited on a Si/SiO_2 substrate. Thermal cycling from 300 K to 700 K and then back to 300 K is performed in air using a Linkam THMS temperature-controlled stage, while Raman spectra are taken during the thermal cycling process. The Raman spectra are

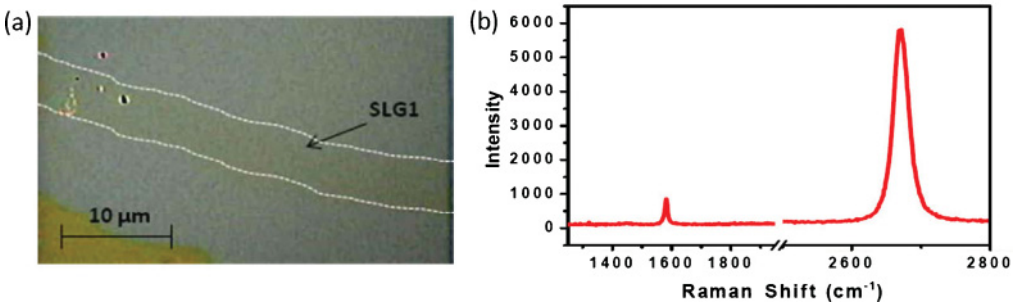

FIG. 1. (Color online) (a) Optical image of SLG1 and (b) Raman spectrum of SLG1.

collected by using a Renishaw spectrometer with a 532-nm laser focused in a 0.5-μm spot through a Leica microscope with a 100× objective lens. The laser power was kept low, at 0.3 mW, during the experiment. The influence of locally heating from the laser is believed to be negligible, since no temperature-induced downshifts of the G band were observed, even when the laser power was increased from 0.3 to 1.5 mW. Raman data taken with different laser powers is presented in the supplementary material online.[27]

III. RESULTS AND DISCUSSION

The G band and $2D$ band Raman spectra of SLG1 taken during thermal cycling are shown in Fig. 2(a) and (b). During heating, the G band Raman shift remains approximately constant while the $2D$ band downshifts monotonically. Since the G band is sensitive to both temperature and doping, the temperature-induced downshift[28] is approximately canceled by the effect doping, which upshifts the mode. The $2D$ band frequency, on the other hand, has a different response to doping and exhibits the expected temperature-induced downshift. During cooling, linear upshifts are observed in both the G and the $2D$ bands, with temperature coefficients of $\partial\omega_G/\partial T = -0.057$ cm^{-1}/K and $\partial\omega_{2D}/\partial T = -0.092$ cm^{-1}/K, respectively, which are slightly higher than those observed in previous works.[9,10,29] By comparing the G and $2D$ band Raman modes before and after thermal cycling (at 300 K), the G band exhibits an irreversible upshift of 24.4 cm^{-1}, whereas the $2D$ band upshifts by 23.2 cm^{-1}. This G band upshift is consistent with our previous work on suspended graphene, which showed a 25 cm^{-1} upshift

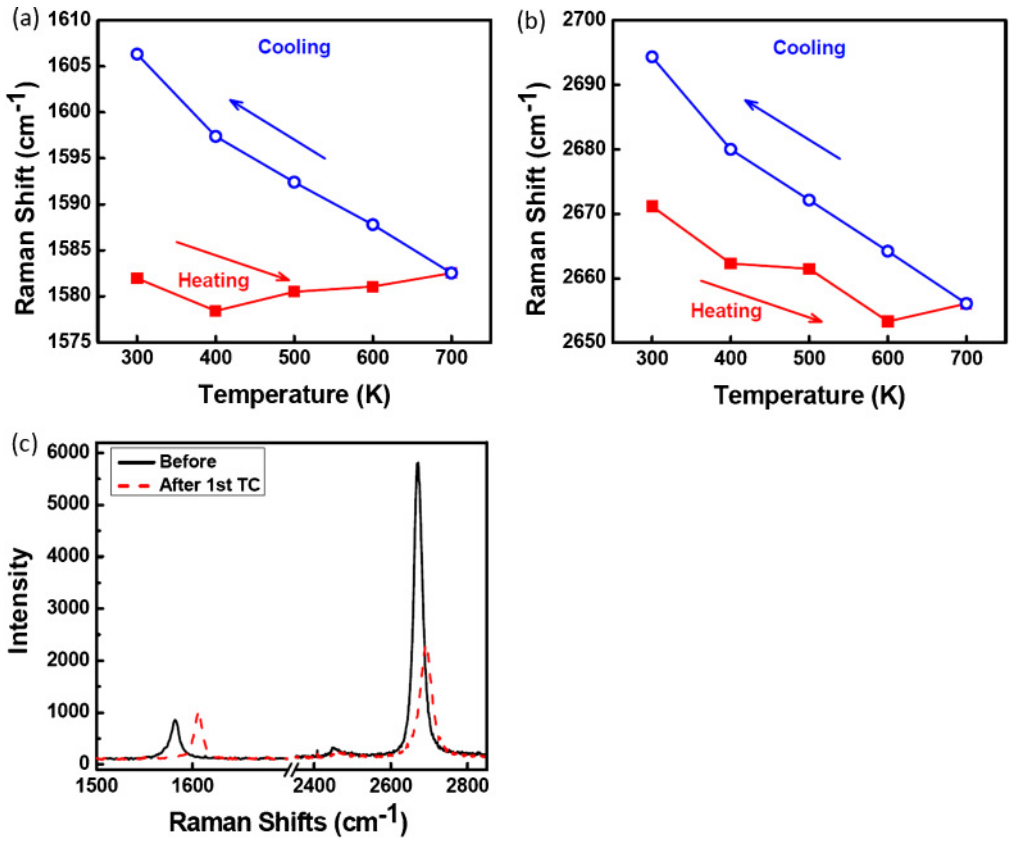

FIG. 2. (Color online) (a) G band and (b) $2D$ band Raman data of SLG taken during the first thermal cycle. (c) Raman spectrum before and after the first thermal cycle (TC).

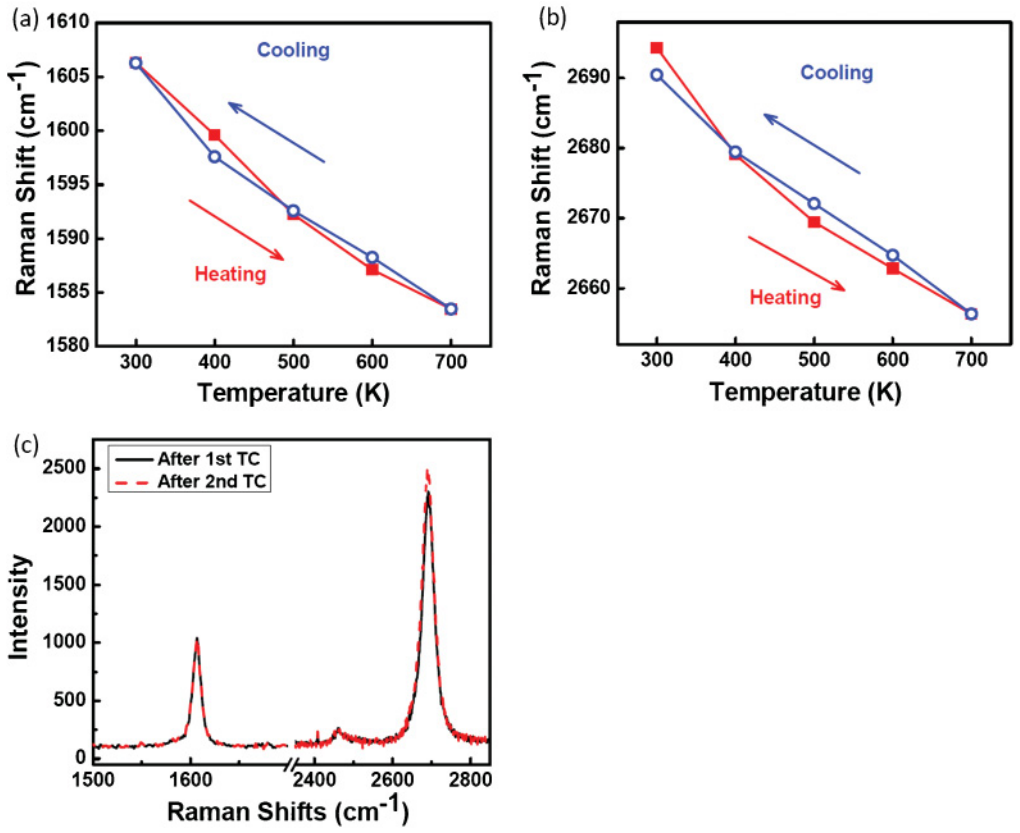

FIG. 3. (Color online) (a) G band and (b) $2D$ band Raman data of SLG taken during the second thermal cycle. (c) Raman spectrum before and after the second thermal cycle (TC).

in the supported region while the suspended region remained constant after thermal cycling.[30] In this previous work, ripple formation in the suspended region of the graphene indicated that the G band upshift originated from the compression of the graphene lattice created by the mismatch of thermal expansion coefficients between the graphene and the underlying Si/SiO_2 substrate.[18,19,31,32] In addition to compression, doping effects can cause the G and $2D$ bands upshifts. Das *et al.* reported G band upshifts of 25 and 7 cm^{-1} linewidth narrowing due to electrostatic doping but $2D$ band upshifts by only 15 cm^{-1} for p-type and downshifts by 20 cm^{-1} for n-type doping.[17] In the experiment presented here, both G and $2D$ bands show similar irreversible upshifts, while the G band full width at half maximum narrowing is less than 2 cm^{-1} after thermal cycling. These results indicate that, in addition to substrate-induced doping effects, a significant amount of compression is created.

A second thermal cycle was carried out on the same sample (SLG1) to 700 K and back to 300 K. The Raman G and $2D$ bands taken during the second thermal cycle are shown in Fig. 3(a) and (b). In the second thermal cycle, the Raman G and $2D$ bands downshift linearly with increasing temperature and upshift linearly to their original frequencies reversibly after cooling to 300 K. Here, we observe Raman temperature coefficients of $\partial\omega_G/\partial T = -0.055$ cm^{-1}/K and $\partial\omega_{2D}/\partial T = -0.083$ cm^{-1}/K. No irreversible upshifts or downshifts of the G or $2D$ bands are observed after the second thermal cycle. This implies that no further compression or doping has occurred in the graphene and that these coefficients represent the *true* temperature dependence of the G and $2D$ bands. Many previous works have measured the temperature coefficients of graphene[9,10,29]; however, the temperature coefficients reported from the previous works are not consistent with one another and span a range from -0.016 to -0.035 cm^{-1}/K for the G band frequency. If we use our initial "heating" data in Fig. 2(a), we obtain a value comparable to those in the literature: -0.034 cm^{-1}/K. However, the Raman spectra observed before and after thermal cycling exhibit irreversible upshifts of the G band after the thermal cycle is complete, which must be taken into consideration when estimating the temperature coefficients of graphene. Both heating and cooling processes are discussed in our experiment.

After thermal cycling, we identify the substrate-induced compression and doping effects, which cause the large irreversible upshifts of the G band. These irreversible upshifts are included in our estimation of the temperature coefficients. Furthermore, the temperature coefficients established in this way are repeatable within the temperature range of thermal cycling and are observed consistently during subsequent heating and cooling processes.

To confirm the assumption that no further compression is induced in the graphene after the first thermal cycle, a triple layer graphene (TLG) flake suspended across a 3-μm trench, shown in Fig. 4(c), was thermally cycled twice to 700 K while observing its Raman spectra. Figure 4(a) shows the height profiles of the suspended TLG measured by AFM before and after the first thermal cycle, which exhibits uniform

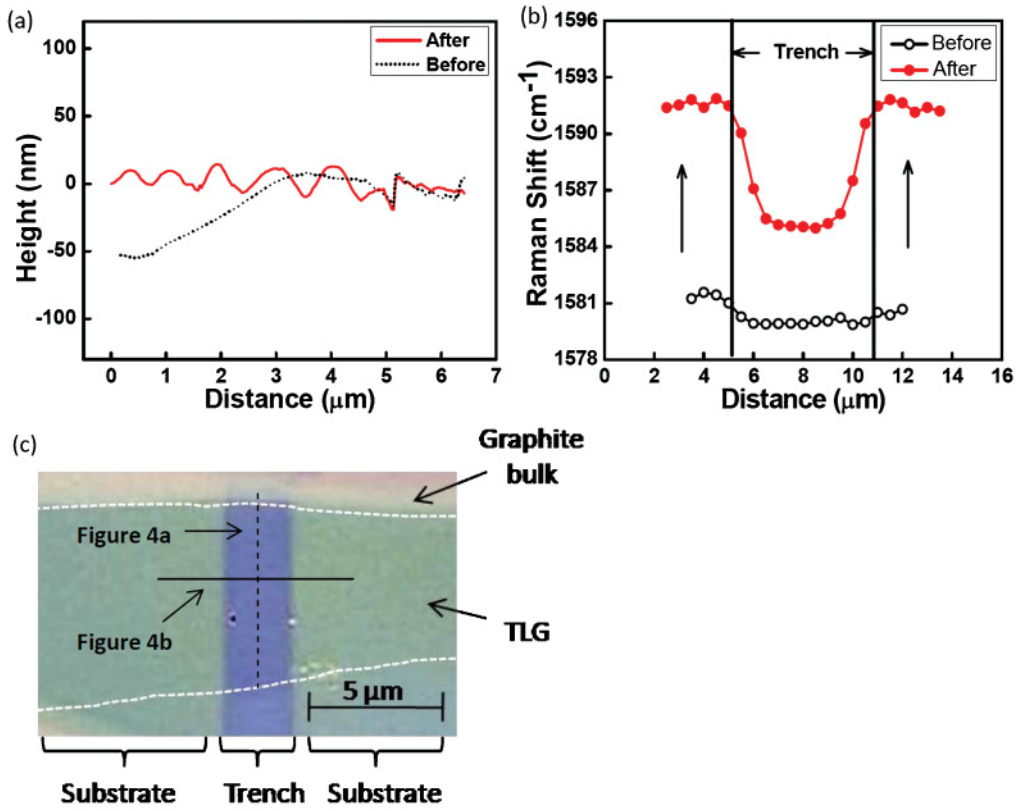

FIG. 4. (Color online) (a) AFM height profile of suspended TLG before and after thermal cycling. (b) Spatially mapped Raman spectral data of the TLG before and after thermal cycling. (c) Optical microscope image of the suspended TLG sample.

and periodic ripples after the first thermal cycle, indicative of compression. Spatially mapped G band shifts taken before and after the first thermal cycle are shown in Fig. 4(b). G band upshifts of 9 and 4 cm^{-1} are observed in the supported and suspended regions, respectively. The magnitudes of these shifts are consistent with our previous work obtained for TLG.

After a second thermal cycle to 700 K, this TLG sample exhibited only slight variations in the amplitude and wavelength of the ripples and in the spatially mapped Raman spectra, as shown in Fig. 5. The consistency of these results before and after the second thermal cycle confirms that no further compression or doping is induced after the first thermal cycle.

We also measured the effect of sequential thermal cycling to incrementally higher temperatures. Another single layer graphene sample (SLG2) was thermally cycled first to 500 K, then to 600 K, and finally to 700 K. Figure 6 shows the G and $2D$ band Raman data taken during these three thermal cycles. For the first thermal cycle to 500 K, the G band shows an initial upshift during the heating process but the $2D$ band does not. This phenomenon can be attributed to the

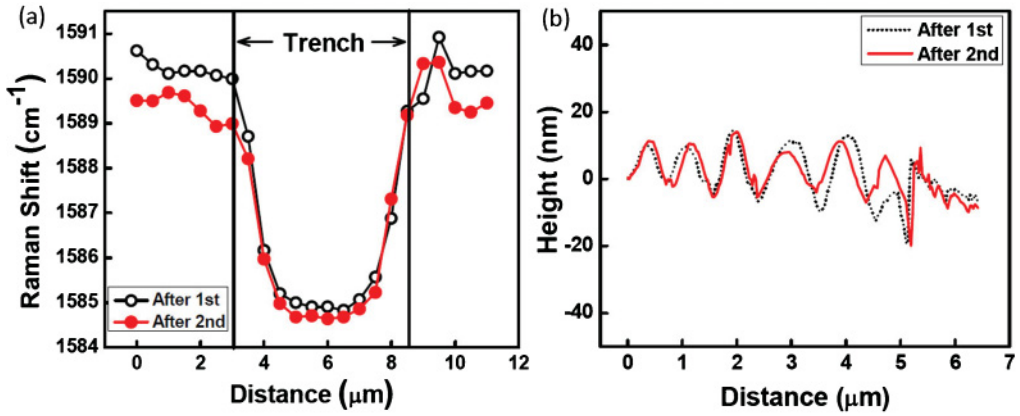

FIG. 5. (Color online) (a) Spatially mapped Raman spectral data and (b) AFM height profile of the bilayer graphene show in Fig. 4 before and after the second thermal cycle to 700 K.

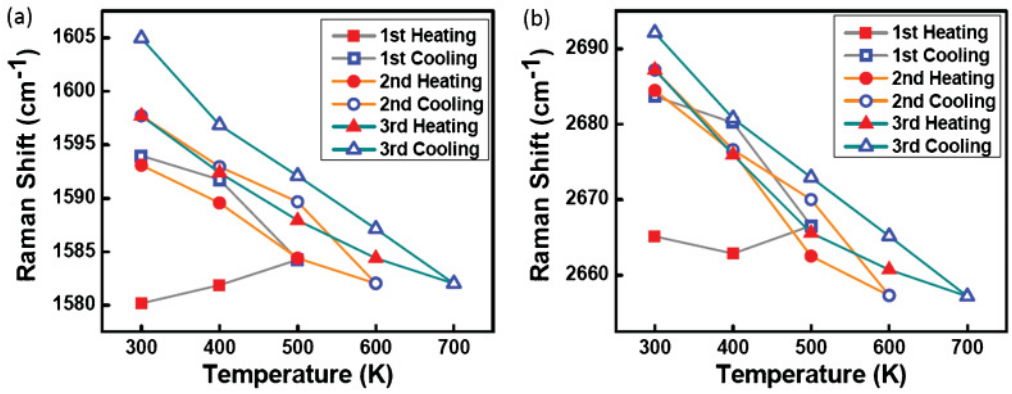

FIG. 6. (Color online) (a) G band and (b) $2D$ band Raman data of SLG taken during three thermal cycles to 500 K, 600 K, and 700 K.

doping effect from the surrounding air and H_2O molecules attaching to the graphene surface. In addition, amorphous SiO_2, which contains a significant density of surface states, can donate electrons to the graphene layer to balance the chemical potential of the graphene–SiO_2 interface.[21] In Fig. 6, the room temperature positions of both the G and the $2D$ bands are observed to upshift after every subsequent thermal cycle. After the third thermal cycle to 700 K, net upshifts of 25 cm^{-1} for the G band and 27 cm^{-1} for the $2D$ band are observed, which are consistent with the upshifts of SLG1 shown in Fig. 1(a) after a single thermal cycling to 700 K. This observation confirms that the equilibrium between the graphene and the underlying Si/SiO_2 substrate is not broken until the graphene is taken to a higher temperature. For this sample, the Raman temperature coefficients of the G and $2D$ bands are $\partial\omega_G/\partial T = -0.055$ and $\partial\omega_{2D}/\partial T = -0.085$ cm^{-1}/K, respectively, during the third cooling process, which are also consistent with the previous results.

In this work, we attribute the irreversible upshifts observed in the Raman spectra to in-plane compression and doping effects in the graphene.[33,34] The in-plane compression effects can also be studied through the observation of ripple formation in suspended graphene, and the doping level in SLG samples can be studied by observing the Raman intensity ratio of the $2D$ and G bands (I_{2D}/I_G). This intensity ratio reduces with increasing carrier concentration.[35,36] Malard *et al.* also thermally cycled on-substrate SLG to 515 K in Ar. In their experiment, no significant $2D$ band upshifts were observed, and all G band upshifts and I_{2D}/I_G Raman intensity ratio changes were attributed to doping alone.[37] Figure 7 shows the intensity ratio of the $2D$ and G bands of SLG1 shown in Figs. 1 and 2 taken during the first and second thermal cycles. This data indicates that the doping effects from the surrounding air molecules and underlying substrate cause a reduction by a factor of five in the relative intensity of the $2D$ band after the first thermal cycle, while the variation of the intensity ratio after the second thermal cycle is negligible. These results imply that SLG1 is doped during the first thermal cycle only.[17,38] However, Malard *et al.* did not observe any significant upshifts in the $2D$ band Raman mode in their thermally cycled graphene. In our work, on the other hand, both Raman G and $2D$ bands upshifted after thermal cycling. The Raman $2D$ band upshifts further confirm the substrate-induced compression on graphene, since graphene is n-type doped after being annealed in vacuum, as reported by Romero *et al.*, and substrate-induced (n-type) doping would result in a $2D$ band downshift.[17,21] Therefore, the large $2D$ band upshifts observed in this work indicate that substrate-induced compression plays a significant role in thermally cycled graphene.

To further investigate the effects of doping, a fresh single layer graphene sample (SLG3) was thermally cycled to 700 K in an Ar gas environment to reduce the effect of gas doping while the Raman spectra are monitored. The Raman data of SLG3 (not shown) measured in Ar shows that during the cooling process, the Raman temperature coefficients, $\partial\omega_G/\partial T = -0.048$ cm^{-1}/K and $\partial\omega_{2D}/\partial T = -0.080$ cm^{-1}/K, are slightly reduced compared with those in air. Both the G and $2D$ bands still show large irreversible upshifts (21.2 and 27.1 cm^{-1}, respectively) after thermal cycling in Ar. These results prove that the large upshifts observed in both air and Ar are dominated by compression and doping induced by the underlying substrate.

Table I shows a summary of the Raman data of the three SLG samples after thermal cycling to 700 K. In this table, SLG1 and SLG2 show similar temperature coefficients and G and $2D$ band upshifts, even though SLG2 has been cycled sequentially to 500 K, 600 K, and then 700 K. The temperature coefficient of SLG3 is slightly lower than that of SLG1 and

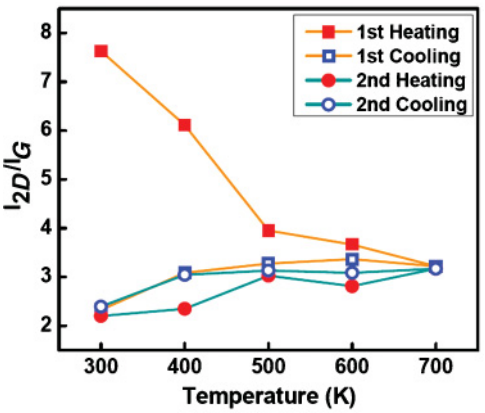

FIG. 7. (Color online) Raman intensity ratio of the $2D$ and G bands taken during the first and second thermal cycles.

TABLE I. Raman data taken on three SLG samples after thermal cycling to 700 K.

	Changes in Raman frequency after 700 K thermal cycling (cm^{-1})					$\frac{\left(\frac{I_{2D}}{I_G}\right)_{Before}-\left(\frac{I_{2D}}{I_G}\right)_{After}}{\left(\frac{I_{2D}}{I_G}\right)_{Before}}$		Raman temperature coefficient (K^{-1})	
	G band		$2D$ band						
Sample	1st cycle	2nd cycle	1st cycle	2nd cycle	Gas	1st cycle	2nd cycle	$\partial\omega_G/\partial T$	$\partial\omega_{2D}/\partial T$
SLG1	24.4	−0.03	23.2	−3.86	Air	0.69	−0.086	−0.055	−0.083
SLG2	24.8	NA	26.9	NA	Air	0.69	NA	−0.055	−0.085
SLG3	21.3	NA	27.2	NA	Ar	0.42	NA	−0.048	−0.080

NA, not applicable.

SLG2. The lower I_{2D}/I_G variation of SLG3 after 700 K thermal cycling indicates that the gas doping effect is reduced by the Ar atmosphere.

IV. CONCLUSIONS

In conclusion, G band and $2D$ band upshifts of 24 and 23 cm^{-1} were observed after thermal cycling SLG to 700 K. These upshifts are attributed to the compression of the graphene induced from the underlying SiO_2/Si substrate and doping effects from the trapped charges in the underlying substrate. No irreversible upshifts were observed after a second thermal cycle to 700 K, indicating that no further compression or doping is induced after the first thermal cycle. By separating the effects of doping, compression, and temperature in graphene, through the interpretation of the resulting Raman spectra, we are able to determine the true temperature dependence of the G and $2D$ bands. Repeatable Raman temperature coefficients are observed after the first thermal cycle, giving SLG Raman temperature coefficients of the G and $2D$ bands of $\partial\omega_G/\partial T = -0.055\ cm^{-1}/K$ and $\partial\omega_{2D}/\partial T = -0.085\ cm^{-1}/K$, respectively. These results provide more complete understanding of the graphene–substrate interaction, which can result in significant variations of graphene's electrical, mechanical, and optical properties.

ACKNOWLEDGMENTS

This research was supported in part by Department of Energy Award No. DE-FG02-07ER46376, Office of Naval Research Award No. N000141010511, and National Science Foundation Award No. CBET-0854118. W.B., Z.Z. and C.N.L. acknowledge the support by NSF CAREER DMR/0748910, ONR N00014-09-1-0724, ONR/DMEA H94003-10-2-1003 and the FENA Focus Center.

*chunchuc@usc.edu

[1] I. Calizo, A. A. Balandin, W. Bao, F. Miao, and C. N. Lau, Nano Lett. **7**, 2645 (2007).
[2] I. Calizo, F. Miao, W. Bao, C. N. Lau, and A. A. Balandin, Appl. Phys. Lett. **91**, 071913 (2007).
[3] M. J. Allen, J. D. Fowler, V. C. Tung, Y. Yang, B. H. Weiller, and R. B. Kaner, Appl. Phys. Lett. **93**, 193119 (2008).
[4] I. Calizo, S. Ghosh, W. Z. Bao, F. Miao, C. N. Lau, and A. A. Balandin, Solid State Commun. **149**, 1132 (2009).
[5] L. J. Ci, Z. P. Zhou, L. Song, X. Q. Yan, D. F. Liu, H. J. Yuan, Y. Gao, J. X. Wang, L. F. Liu, W. Y. Zhou, G. Wang, and S. S. Xie, Appl. Phys. Lett. **82**, 3098 (2003).
[6] Z. H. Ni, T. Yu, Y. H. Lu, Y. Y. Wang, Y. P. Feng, and Z. X. Shen, ACS Nano **3**, 483 (2009).
[7] J. J. Lin, L. W. Guo, Q. S. Huang, Y. P. Jia, K. Li, X. F. Lai, and X. L. Chen, Phys. Rev. B **83**, 125430 (2011).
[8] C. C. Chang, I. K. Hsu, M. Aykol, W. H. Hung, C. C. Chen, and S. B. Cronin, ACS Nano **4**, 5095 (2010).
[9] D. J. Late, U. Maitra, L. S. Panchakarla, U. V. Waghmare, and C. N. R. Rao, J. Phys. Condens. Matter **23**, 055303 (2011).
[10] D. Abdula, T. Ozel, K. Kang, D. G. Cahill, and M. Shim, J. Phys. Chem. C **112**, 20131 (2008).
[11] T. Yu, Z. H. Ni, C. L. Du, Y. M. You, Y. Y. Wang, and Z. X. Shen, J. Phys. Chem. C **112**, 12602 (2008).
[12] M. Y. Huang, H. G. Yan, T. F. Heinz, and J. Hone, Nano Lett. **10**, 4074 (2010).
[13] M. Y. Huang, H. G. Yan, C. Y. Chen, D. H. Song, T. F. Heinz, and J. Hone, Proc. Nat. Acad. Sci. USA **106**, 7304 (2009).
[14] N. Ferralis, J. Mater. Sci. **45**, 5135 (2010).
[15] T. M. G. Mohiuddin, A. Lombardo, R. R. Nair, A. Bonetti, G. Savini, R. Jalil, N. Bonini, D. M. Basko, C. Galiotis, N. Marzari, K. S. Novoselov, A. K. Geim, and A. C. Ferrari, Phys. Rev. B **79**, 205433 (2009).
[16] A. C. Ferrari, Solid State Commun. **143**, 47 (2007).
[17] A. Das, S. Pisana, B. Chakraborty, S. Piscanec, S. K. Saha, U. V. Waghmare, K. S. Novoselov, H. R. Krishnamurthy, A. K. Geim, A. C. Ferrari, and A. K. Sood, Nat. Nanotech. **3**, 210 (2008).
[18] N. Mounet and N. Marzari, Phys. Rev. B **71**, 205214 (2005).
[19] V. Singh, S. Sengupta, H. S. Solanki, R. Dhall, A. Allain, S. Dhara, P. Pant, and M. M. Deshmukh, Nanotechnology **21**, 209801 (2010).
[20] W. Z. Bao, F. Miao, Z. Chen, H. Zhang, W. Y. Jang, C. Dames, and C. N. Lau, Nat. Nanotech. **4**, 562 (2009).
[21] H. E. Romero, N. Shen, P. Joshi, H. R. Gutierrez, S. A. Tadigadapa, J. O. Sofo, and P. C. Eklund, ACS Nano **2**, 2037 (2008).
[22] K. S. Novoselov, S. V. Morozov, T. M. G. Mohinddin, L. A. Ponomarenko, D. C. Elias, R. Yang, I. I. Barbolina, P. Blake, T. J. Booth, D. Jiang, J. Giesbers, E. W. Hill, and A. K. Geim, Phys. Status Solidi B **244**, 4106 (2007).

[23] A. H. Castro Neto, F. Guinea, N. M. R. Peres, K. S. Novoselov, and A. K. Geim, Rev. Mod. Phys. **81**, 109 (2009).
[24] A. Gupta, G. Chen, P. Joshi, S. Tadigadapa, and P. C. Eklund, Nano Lett. **6**, 2667 (2006).
[25] A. C. Ferrari, J. C. Meyer, V. Scardaci, C. Casiraghi, M. Lazzeri, F. Mauri, S. Piscanec, D. Jiang, K. S. Novoselov, S. Roth, and A. K. Geim, Phys. Rev. Lett. **97**, 187401 (2006).
[26] L. M. Malard, M. A. Pimenta, G. Dresselhaus, and M. S. Dresselhaus, Phys. Rep. **473**, 51 (2009).
[27] See Supplemental Material at http://link.aps.org/supplemental/10.1103/PhysRevB.85.035431 for Raman data taken with different laser powers.
[28] H. Zhou, C. Qiu, F. Yu, H. Yang, M. Chen, L. Hu, Y. Guo, and L. Sun, J. Phys. D: Appl. Phys. **44**, 185404 (2011).
[29] L. Zhang, Z. Jia, L. M. Huang, S. O'Brien, and Z. H. Yu, J. Phys. Chem. C **112**, 13893 (2008).
[30] C. C. Chen, W. Z. Bao, J. Theiss, C. Dames, C. N. Lau, and S. B. Cronin, Nano Lett. **9**, 4172 (2009).
[31] H. Tada, A. E. Kumpel, R. E. Lathrop, J. B. Slanina, P. Nieva, P. Zavracky, I. N. Miaoulis, and P. Y. Wong, J. Appl. Phys. **87**, 4189 (2000).
[32] H. Watanabe, N. Yamada, and M. Okaji, Int. J. Thermophys. **25**, 221 (2004).
[33] J. Yan, Y. B. Zhang, P. Kim, and A. Pinczuk, Phys. Rev. Lett. **98**, 166802 (2007).
[34] C. Stampfer, F. Molitor, D. Graf, K. Ensslin, A. Jungen, C. Hierold, and L. Wirtz, Appl. Phys. Lett. **91**, 241907 (2007).
[35] D. M. Basko, S. Piscanec, and A. C. Ferrari, Phys. Rev. B **80**, 165408 (2009).
[36] S. Berciaud, S. Ryu, L. E. Brus, and T. F. Heinz, Nano Lett. **9**, 346 (2009).
[37] L. M. Malard, R. L. Moreira, D. C. Elias, F. Plentz, E. S. Alves, and M. A. Pimenta, J. Phys. Condens. Matter **22**, 334202 (2010).
[38] C. Casiraghi, Phys. Rev. B **80**, 233407 (2009).